JJAP Series 5
Proc. of 1991 Intern. MicroProcess Conference pp. 232–237

Reactive Ion Etching Using Electron Cyclotron Resonance Hydrogen Plasma with n-Butyl Acetate Reactive Gas

Toshihiro MIYATA, Tadatsugu MINAMI, Hirotoshi SATO and Shinzo TAKATA

Electron Device System Laboratory, Kanazawa Institute of Technology, 7-1 Oogigaoka, Nonoichi, Ishikawa 921

(Received July 17, 1991; accepted for publication December 21, 1991)

Electron cyclotron resonance hydrogen plasma reactive ion etching (RIE) with n-butyl acetate reactive gas has been demonstrated. The etching mechanism is discussed for RIE of transparent conducting oxide films. The RIE technique exhibits excellent material selectivity resulting from the ability to control the etching mechanism by altering the accelerating voltage frequency. To demonstrate the practical application of RIE, an electroluminescent display fabrication is described.

KEYWORDS: reactive ion etching, electron cyclotron resonance, transparent conducting films, hydrogen plasma, n-butyl acetate, electroluminescent device

§1. Introduction

In the fabrication of flat panel displays using electroluminescent (EL) devices or liquid crystal (LC) devices, the need for dry processes in the patterning of transparent conducting oxide (TCO) films has been growing in recent years. Dry etching of TCO films using argon ion sputtering[1] and reactive ion etching (RIE) have been reported.[2] However, sputter etching has disadvantages such as low etching selectivity and sputtering-induced damage. In addition, conventional RIE with halogen reactive gases also has disadvantages such as damage to the apparatus and degradation of the films due to the residuum.

Recently, we reported that halogen-free RIE using electron cyclotron resonance (ECR) hydrogen plasma is useful as a method of dry etching TCO films, for example, undoped and fluorine-doped tin oxide (TO and FTO).[3] The etching was enhanced by the use of organic reactive gases, especially, n-butyl acetate. The ECR hydrogen plasma in RIE results in a reduction effect, sputtering of the TCO films and activation of organic reactive gases.[4] On the other hand, RIE using rf (13.56 MHz) plasma with a methyl alcohol reactive gas in the patterning of indium tin oxide (ITO) films resulted in poor etching selectivity because of the absence of a hydrogen plasma source.[5,6]

In this paper, we have described the etching selectivity of RIE using an ECR hydrogen plasma with an n-butyl acetate reactive gas. To demonstrate the practical application of ECR hydrogen plasma RIE, EL display fabrication is also described.

§2. Experimental Procedure

The ECR hydrogen plasma RIE of TCO films was carried out on commercially available FTO, ITO and aluminum-doped zinc oxide (AZO) films. The FTO (Central Glass Co.) films were formed on a heated (about 550°C) glass substrate (thickness of about 5 mm) by a chemical vapor deposition (CVD) method. The ITO and AZO films[7] were formed using magnetron sputtering methods on glass substrates (thickness of about 1.1 mm) heated above 200°C. The thickness, resistivity and preparation method of these TCO films are listed in Table I. In order to investigate etching selectivity for other materials, ECR hydrogen plasma RIE was also carried out on phosphor films and insulating oxide films. The ZnS:Mn film (thickness of about 400 nm) and CaS, SrS, SiO_2, Al_2O_3 and Ta_2O_5 films (thickness of about 500 nm) were prepared on the glass substrates (thickness of about 1.1 mm) by organometallic chemical vapor deposition (OMCVD)[8] and rf magnetron sputtering, respectively.

Figure 1 shows the ECR hydrogen plasma RIE system used in this study. This apparatus consists of the ECR plasma chamber and etching chamber. An accelerating electrode (mesh configuration) and sample holder, separated by a distance of 10 cm, were set at the exit of the ECR plasma chamber and in the etching chamber, respectively. In the plasma chamber, the ECR hydrogen plasma was generated with a microwave power of about 300 W at 2.45 GHz under an applied magnetic field of 8.75×10^{-2} T. An ac accelerating voltage with a frequency of 15 kHz, 380 kHz or 13.56 MHz was applied between the accelerating electrode and the sample holder with a power density of about 11, 3 or 2 W/cm^2, respectively. The hydrogen plasma was introduced into the etching chamber under the influence of both the divergence

Table I. The thickness, resistivity and preparation methods of FTO, ITO and AZO films used in this work.

	SnO_2:F (FTO)	In_2O_3:Sn (ITO)	ZnO:Al (AZO)
Thickness (nm)	540	120	120
Resistivity $\rho(\Omega \cdot cm)$	5.0×10^{-4}	2.0×10^{-4}	3.0×10^{-4}
Deposition Method	CVD	Sputter	Sputter

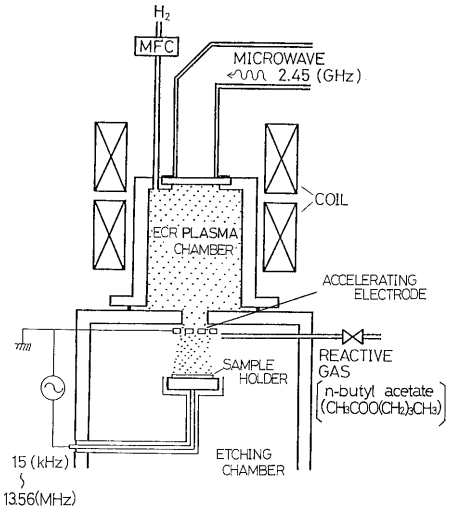

Fig. 1. Schematic diagram of the reactive ion etching system using ECR hydrogen plasma.

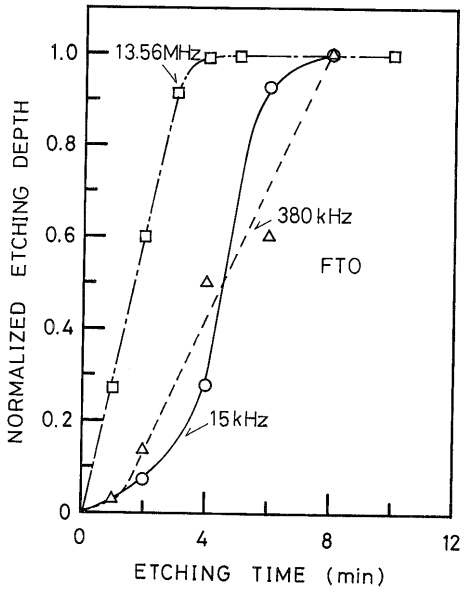

Fig. 2. The normalized etching depth of FTO films as a function of etching time for three accelerating frequencies: 15 kHz (○), 380 kHz (△) and 13.56 MHz (□).

magnetic field and the accelerating electric field. The n-butyl acetate ($CH_3COO(CH_2)_3CH_3$) reactive gas, after injection into the etching chamber, was activated by the hydrogen ions and radicals coming from the ECR plasma chamber. The total pressure of the reactive gas and the hydrogen gas mixture was 6.65×10^{-1} Pa. The thickness of the films was measured by a conventional stylus-type surface roughness detector.

§3. Results and Discussion

3.1 *Relationship between TCO film etching characteristics and accelerating voltage frequency*

In the ECR hydrogen plasma RIE of TCO films, the time dependencies of etching depth and etching rate were strongly a function of the TCO material, the reactive gas pressure and the frequency of the accelerating voltage. In the case of FTO films using RIE with different accelerating frequencies, the normalized etching depth as a function of etching time is shown in Fig. 2. The normalized etching depth in this figure refers to the ratio of the etched depth to the film thickness before etching for an etching time of 5 min. The ratio of reactive gas (n-butyl acetate) pressure to total pressure was 0.4. With a high accelerating voltage frequency of 13.56 MHz, the etched depth linearly increases with etching time. However, at lower frequencies, the etching rate is initially low.

The normalized etching rate of FTO films as a function of the ratio of n-butyl acetate pressure to total pressure is shown in Fig. 3 for accelerating frequencies of 15 kHz and 13.56 MHz. In this figure, the normalized etching rate refers to the ratio of the etched depth, with and without the n-butyl acetate reactive gas for an etching time of 5 min. The maximum etching rates of 127 nm/min at 13.56 MHz and 57 nm/min at 15 kHz were obtained at an n-butyl acetate gas pressure ratio of about 40% (data not shown). It should be noted in Fig. 3 that the maximum normalized etching rate at 15 kHz was larger than that at 13.56 MHz, whereas the etching rate for an accelerating frequency of 13.56 MHz was larger than that for 15 kHz. These results indicate that the introduction of a reactive gas is more effective at an accelerating frequency of 15 kHz than at 13.56 MHz and that the etching mechanism of FTO films is a function of the accelerating frequency.

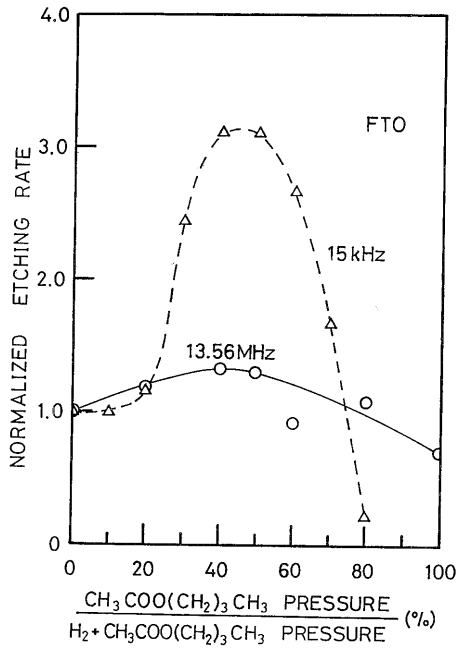

Fig. 3. The normalized etching rate of FTO films as a function of the ratio of n-butyl acetate pressure to total pressure for two accelerating frequencies: 15 kHz (△), and 13.56 MHz (○).

The etching characteristics for other TCO film materials, such as ITO and AZO, were also investigated in detail using RIE with different accelerating frequencies. The normalized etching depth of ITO and AZO films as a function of etching time are shown in Figs. 4 and 5, respectively, for RIE with different accelerating

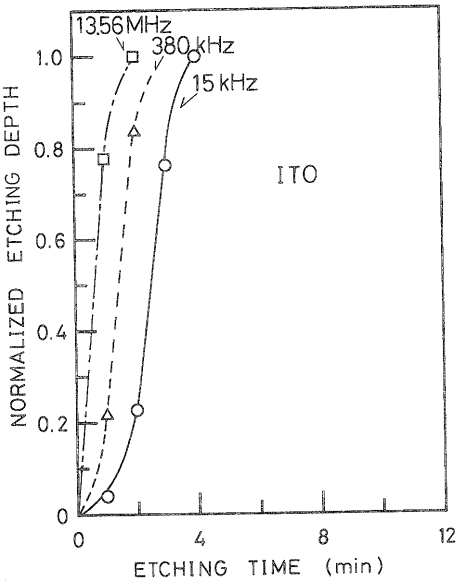

Fig. 4. The normalized etching depth of ITO films as a function of etching time for three accelerating frequencies: 15 kHz (○), 380 kHz (△) and 13.56 MHz (□).

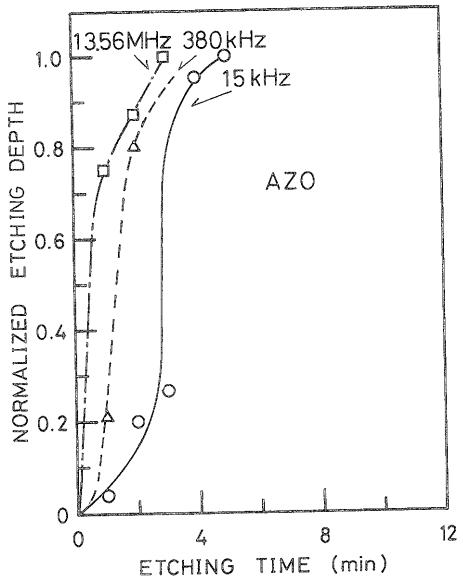

Fig. 5. The normalized etching depth of AZO films as a function of etching time for three accelerating frequencies: 15 kHz (○), 380 kHz (△) and 13.56 MHz (□).

frequencies. As seen in these figures, the normalized etching depth characteristics of these films are similar to that of FTO, as shown in Fig. 3. Figure 6 shows a rise in etching rate with increasing accelerating frequency for three TCO films: FTO, ITO and AZO, listed in descending order of etching rate.

3.2 *Etching characteristics of other thin films*

In fabricating conventional LC or thin-film EL (TFEL) displays, etching selectivity between the transparent electrode or the emitting layer and the insulating layer is generally required. Manganese-doped

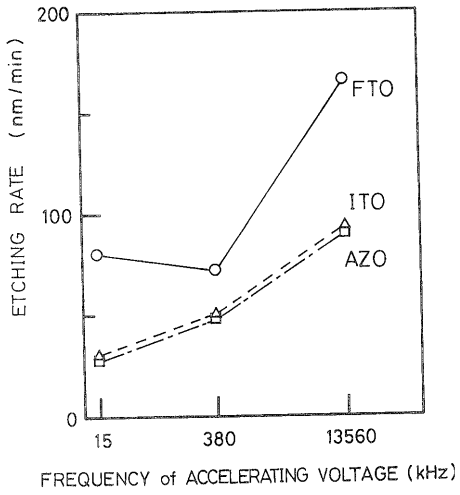

Fig. 6. The accelerating frequency dependence of the etching rate for FTO (○), ITO (△) and AZO (□) films.

zinc sulfide (ZnS:Mn) and silicon dioxide (SiO_2) thin films have been used practically as the emitting layer and the insulating layer, respectively, in many TFEL displays. The normalized etching depths of ITO, ZnS:Mn and SiO_2 films as a function of etching time are shown in Fig. 7 for an accelerating frequency of 15 kHz; Fig. 8 shows the accelerating frequency dependence of the etching rate of these films for an etching time of 5 min. Although all of these films experienced RIE at 13.56 MHz, the SiO_2 film was not etched when the frequency was low, 15 kHz. We also found that emitting layers such as CaS and SrS films were also unetched when the frequency was 15 kHz. In addition, insulating layers such as $BaTiO_3$, Al_2O_3 and Ta_2O_3 exhibited the same frequency dependence of etching as the SiO_2, CaS and SrS films. These results suggest that etching selectivity can be

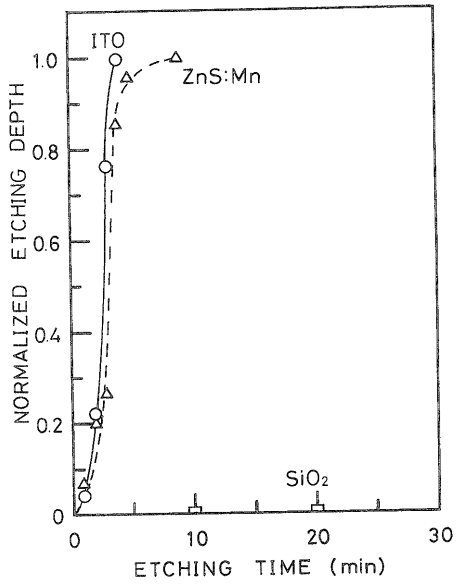

Fig. 7. The dependence of the normalized etching depth of ITO (○), ZnS:Mn (△) and SiO_2 (□) films on the etching time using RIE with an accelerating frequency of 15 kHz.

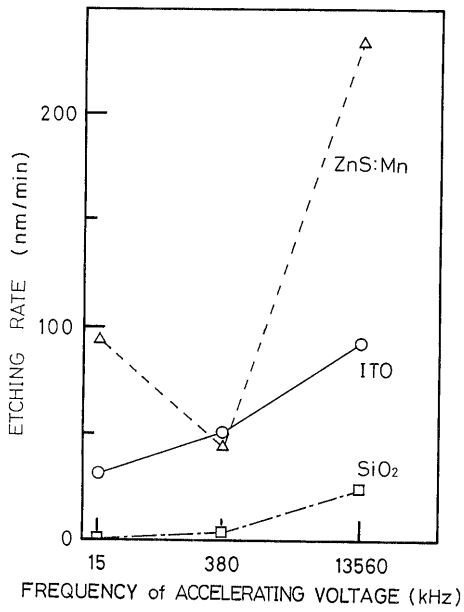

Fig. 8. The accelerating frequency dependence of the etching rate for ITO (○), ZnS:Mn (△) and SiO_2 (□) films.

controlled by varying the frequency of the accelerating voltage in ECR hydrogen plasma RIE.

3.3 *Etching mechanism*

We have proposed the following etching mechanisms to describe the RIE (with an accelerating frequency of 15 kHz) of TO or FTO films using ECR hydrogen plasma with organic reactive gases.[4] The films are chemically reduced by active hydrogen, ions and radicals from the ECR hydrogen plasma, as evidenced by the coloring of the films and the lower etching rate in the initial stage of etching. Subsequently, the reduced tin oxide films which became metal-rich films may be removed by both the sputtering due to hydrogen ions and the production of the tin hydride. In the presence of n-butyl acetate reactive gas, chemically active methyl and ethyl ions and radicals, generated from n-butyl acetate decomposed by the activated hydrogen in the plasma chamber, also react with the metallic tin atoms which are produced by the reducing effect of the ECR hydrogen plasma, and tin alkyls such as methyl and ethyl are formed. In addition, the sputtering of tin-rich films may be enhanced by the ions generated from decomposed n-butyl accetate. Consequently, these enhance the removal of metallic tin atoms from the substrate.

On the other hand, it was found in this work that only when films were reduced by ECR hydrogen plasma, were they etched by RIE at 15 kHz. This suggests that the chemical reducing effect of films predominates RIE at 15 kHz. On the contrary, all of the films used were etched by RIE at 13.56 MHz. In addition, all of the films used in this work were easily etched by RIE with an accelerating frequency of 13.56 MHz using argon ECR plasma without the reactive gas, whereas at 15 kHz, all films were unetched. These results suggest that physical sputtering is enhanced in RIE at a high accelerating frequency.

Therefore, the accelerating-frequency-dependent etching characteristics described above suggest that etching selectivity is related to differences in the etching mechanism. This relationship is attributed to the generation of a dc self-bias caused by the velocity differential between electrons and ions in the plasma. The dc self-bias was absent at an accelerating frequency of 15 kHz, as evidenced from the calculated movable distance of hydrogen ions for a half-cycle of accelerating voltage. However, with a high accelerating frequency of 13.56 MHz, the dc self-bias is generated because the movable distance of hydrogen ions is shorter than the distance between the sample holder and the accelerating electrode.

The results indicate that ECR hydrogen plasma RIE includes both physical and chemical etching mechanisms; i.e., at high accelerating voltage frequencies, physical etching is significantly enhanced, whereas at low frequencies, chemical etching predominates. At an intermediate frequency of 380 kHz, physical etching and chemical etching compete. Therefore, differences in the etching rate obtained for all thin films used in this work are explained by the relative ease of their reduction in the hydrogen plasma and the sputter yield of the films.

3.4 *Application to TFEL display fabrication*

Recently, we reported a TFEL device using a ferroelectric ceramic sheet acting as the insulating layer as well as the substrate (ICTFEL device).[9] Previous studies have clarified that ICTFEL devices have the following features: low operating voltage and high luminance under low-frequency driving.[9,10]

The patterning in the fabricated ICTFEL display was carried out by the following procedures, as shown in Fig. 9. A conducting AZO layer in a row strip pattern was inserted between the $BaTiO_3$ ceramic and ZnS:Mn emitting layers to eliminate crosstalk between pixels.[11] This same process was used in patterning the back electrode row strip. The strip mask pattern was formed on the AZO transparent electrode using photoresist (OFPR 800). The AZO transparent electrode and ZnS:Mn emitting layer were etched by ECR hydrogen plasma RIE with an accelerating frequency of 15 kHz. The pressure ratio of the n-butyl acetate reactive gas to total gas pressure was 0.4. After etching, the photoresist was ashed by using rf (13.56 MHz) oxygen plasma.

In these patterning procedures, it was difficult to avoid

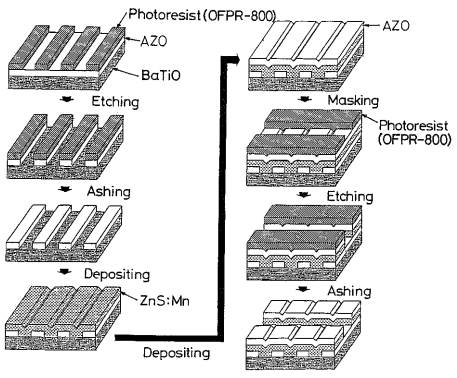

Fig. 9. Patterning procedures for a TFEL display using an ICTFEL device.

damage due to chemical reactions such as a slightly reduced surface of the $BaTiO_3$ ceramic insulating layer; however, we found that this reduced surface could recover when post-oxidation was used. In the postoxidation process, the reduced $BaTiO_3$ ceramic was exposed to the ECR oxygen plasma generated in the same chamber postetching. Thus, after etching of the AZO films, the $BaTiO_3$ ceramic surface was always oxidized using ECR oxygen plasma.

We have studied the stability of unintentionally heated TCO films when exposed to oxygen plasma, as in the oxidizing and ashing processes. Figure 10 shows resistivity (ρ), carrier concentration (n) and Hall mobility (μ) of AZO films prepared at different substrate temperatures, before and after exposure to ECR oxygen plasma. As seen in this figure, these electrical characteristics were unchanged by the exposure. It was also found that all TCO films used in this work were stable when exposed to ECR or rf oxygen plasma.

Figure 11 is a photograph of a 3-figure segment display composed of ICTFEL devices with a 7-segment-pattern ZnS:Mn emitting layer and AZO transparent electrode. We also fabricated a 9×10 dot-matrix display using an ICTFEL device which consists of column strip patterns of the multilayer with ZnS:Mn film and AZO film and

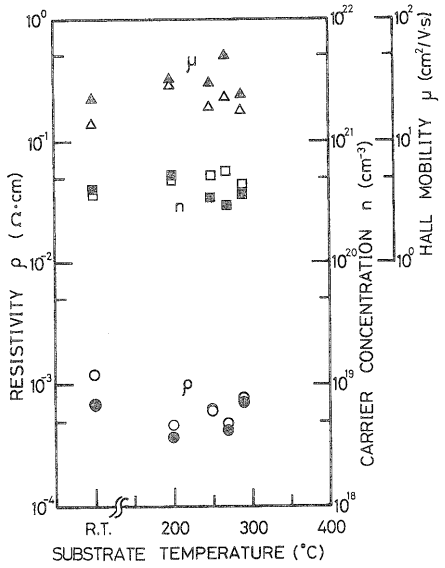

Fig. 10. The resistivity ρ(○), carrier concentration n(□) and Hall mobility μ(△) of AZO films prepared at different substrate temperatures, before (solid) and after (open) exposure to ECR oxygen plasma.

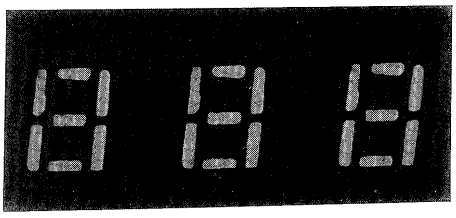

Fig. 11. A photograph of a three-figure segment display fabricated by ICTFEL devices with seven-segment pattern.

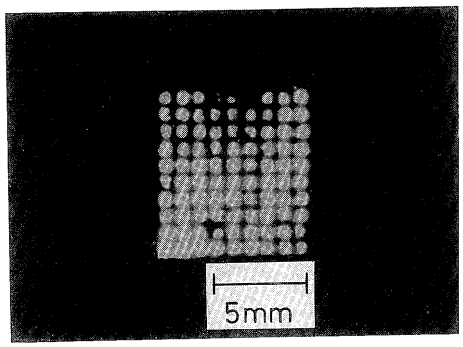

Fig. 12. A photograph of a 9×10 dot-matrix display using an ICTFEL device.

back electrode row strip patterns, as shown in Fig. 12.

§4. Conclusions

A halogen-free RIE technique using a ECR hydrogen plasma with n-butyl acetate reactive gas was demonstrated. Excellent material etching selectivity was obtained, and the etching selectivity could be controlled by varying the frequency of the accelerating voltage. It was found that this alteration of the accelerating voltage frequency changed the etching mechanism of the RIE of TCO films. At high accelerating voltage frequencies, physical sputtering was enhanced in RIE, whereas at low frequency of 15 kHz, chemical etching predominated. This accelerating frequency dependence of etching selectivity is explained by a dc self-bias which is related to changes in the movable distance of ions. Also, segment and dot-matrix TFEL displays were successfully fabricated using this excellent etching selectivity. Thus, we can conclude that the RIE technique, which is free from damage to the apparatus and degradation of films caused by residuum, is also very useful for the fabrication of optoelectronic devices.

Acknowledgments

The authors wish to acknowledge A. Iwamoto, S. Abe, H. Kitagata, H. Wakuda, R. Takayanagi, K. Miyamoto, H. Miyake, S. Tamura, T. Kokubun, T. Goto and M. Tsuzi for their technical assistance in the experiments. The authors are also grateful to Central Glass Co., Ltd. for preparation of the FTO films and $BaTiO_3$ fine powder.

References

1) C. Brunel, N. Bouadma and P. Le Berre: *Proc. Eurodisplay 87, London, 1987* (Society for Information Display, London, 1987) p. 238.
2) P. Maguire, J. Shields, J. Mclaughlin, J. Anderson and S. Laverty: *Proc. 9th Int. Display Research Conf., Kyoto, 1989* (Society for Imformation Display, Kyoto, 1989) p. 62.
3) T. Minami, H. Sato, H. Nanto and S. Takata: *Abstracts of 7th Int. Conf. on Thin Films, New Delhi India, 1987*, p. 226. [Thin Solid Films **176** (1989) 227.]
4) T. Minami, T. Miyata, A. Iwamoto, S. Takata and H. Nanto: Jpn. J. Appl. Phys. **27** (1988) L1753.
5) T. Kawaguchi, E. Takeda, Y. Nanno and S. Nagata: *Proc. 9th Int. Display Research Conf., Kyoto, 1989* (Society for Imformation Display, Kyoto, 1989) PD-1.
6) M. Yamamoto, M. Inoue, T. Tohda, T. Matsuoka and A. Abe:

Proc. 9th Int. Display Research Conf., Kyoto, 1989 (Society for Imformation Display, Kyoto, 1989) p. 228.
7) T. Minami, H. Nanto and S. Takata: Jpn. J. Appl. Phys. **23** (1984) L280.
8) S. Takata, T. Minami, T. Miyata and H. Nanto: J. Cryst. Growth **86** (1987) 257.
9) T. Minami, S. Orito, H. Nanto and S. Takata: *Proc. 6th Int. Display Research Conf., Tokyo, 1986* (Society for Information Display, Tokyo, 1986) p. 140.
10) T. Minami, T. Miyata, K. Kitamura, H. Nanto and S. Takata: Jpn. J. Appl. Phys. **27** (1988) L876.
11) T. Minami, T. Miyata, K. Kitamura, Y. Kusano, S. Takata and H. Nanto: Proc. *9th Int. Display Research Conf., Kyoto, 1989* (Society for Imformation Display, Kyoto, 1989) p. 82.